J Solid State Electrochem (2017) 21:1045–1058
DOI 10.1007/s10008-016-3461-7

ORIGINAL PAPER

Semi-differential analysis of irreversible voltammetric peaks

M. Grdeń [1]

Received: 13 September 2016 / Revised: 27 October 2016 / Accepted: 1 November 2016 / Published online: 10 November 2016

Abstract Voltammetric peaks obtained by simulation of electrochemical reactions under conditions of linear semi-infinite diffusion with an irreversible electron transfer process are analysed using a semi-differentiation procedure. Obtained semi-derivative peaks, separated or overlapped, are fitted with appropriate mathematical functions. The functions used for data fitting include a function describing symmetrical peaks, proposed by several authors for fitting irreversible semi-derivative peaks, and two alternative functions that express asymmetric shape of the irreversible semi-derivative signals. When applied to the overlapped irreversible semi-derivative peaks, the latter two functions allow calculating certain electrochemical parameters with a better accuracy as compared with the function derived for the symmetrical peaks.

Keywords Voltammetry · Semi-differentiation · Voltammetric data fitting · Irreversible electron transfer

Introduction

Mathematical methods based on semi-differentiation and semi-integration offer an interesting alternative to classical analysis of voltammetric curves [1–20]. Various electrochemical processes, such as redox reactions with reduced and oxidised species present in the same phase [6, 14, 21–35], adsorption on surfaces of electrodes [36–38], electrodeposition [39–48] or electrodissolution [49–51] were analysed by means of semi-differentiation or semi-integration. The most extensive mathematical treatment related to these methods was applied to the electrochemical reactions were both oxidised and reduced form are soluble in the electrolyte phase and their transport proceeds under conditions of semi-infinite linear diffusion [4]. The semi-differentiation, which is the subject of this manuscript, allows transformation of strongly asymmetric diffusive current peaks into much more symmetrical, bell-shaped semi-derivative signals with well-defined end [4, 12, 42, 52]. Application of such procedure is very helpful for separation of overlapped voltammetric peaks, the benefits depend on the extent of their overlapping. Thus, obtained semi-derivative peaks could be completely separated or may overlap [2]. Even if overlapped, however, the semi-derivative peaks are usually easier to distinguish as compared with their voltammetric precursors and are more convenient for further evaluation. A further analysis of overlapped semi-derivative signals should include their deconvolution by means of fitting with appropriate mathematical functions derived for a certain type of the electrochemical reaction [2].

An extensive description of the theory of semi-differentiation and semi-integration can be found elsewhere [11, 14, 51, 53–60]; here, we focus only on practical aspects of its application in analysis of voltammetric data for systems with reactions under conditions of semi-infinite linear diffusion and when oxidised and reduced species are soluble in the electrolyte phase. It should be stressed that most of the modern electrochemical software offer a possibility of data transformation using both abovementioned methods making their application easily accessible. The semi-differentiation, i.e. fractional differentiation with the order of 0.5, can be represented for the electrochemical purposes as Eq. (1) [2, 4, 61]:

$$e = \frac{\mathrm{d}^{1/2} i}{\mathrm{d}t^{1/2}} = \pi^{-1/2} \frac{\mathrm{d}}{\mathrm{d}t} \int_0^t \frac{i(\tau)\mathrm{d}\tau}{\sqrt{t-\tau}} \tag{1}$$

where e stands for the semi-derivative, i is the current, t is the time and τ is the integration variable. The final

✉ M. Grdeń
mgrden@chem.uw.edu.pl

[1] Faculty of Chemistry, Biological and Chemical Research Centre, University of Warsaw, Żwirki i Wigury 101, 02-089 Warsaw, Poland

mathematical formulae describing the shape of obtained semi-derivative peaks are different for reversible and irreversible electron transfer reactions [4]. For the reversible case, the following exact mathematical formula was derived (Eq. 2) [4]:

$$e = 0.25An^2\mathrm{F}^2cvD^{1/2}(\mathrm{R}T)^{-1}\left(\cosh\left(0.5n\mathrm{F}\mathrm{R}^{-1}T^{-1}\left(E-E_\mathrm{p}\right)\right)\right)^{-2} \quad (2)$$

where A is the surface area, n is the number of exchanged electrons, c is the concentration of reacting species, v is the potential scan rate, D is the diffusion coefficient, E_p is the peak potential and the other terms have their usual meanings. The semi-derivative peak described by Eq. (2) is completely symmetrical (Fig. 1) [4, 12, 42, 52, 62], the term preceding $\cosh^{-2}$ is equal to the peak height.

A more complicated situation arises for an irreversible electron transfer, when the expression of the semi-derivative peak is given by a series (Eq. 3) which cannot be simplified to a mathematical form more convenient for the further use [4]:

$$e = -\left(A\alpha n^2\mathrm{F}^2cvD^{1/2}(\mathrm{R}T)^{-1}\right)\sum_{i=1}^{\infty}\left((-1)^i i(i!)^{1/2}\exp\left(i\alpha\mathrm{F}n\left(E-E_\mathrm{p}-0.055\mathrm{R}T(\alpha n\mathrm{F})^{-1}\right)(\mathrm{R}T)^{-1}\right)\right) \quad (3)$$

where α is the transfer coefficient or the symmetry factor, depending on the reaction mechanism [63, 64]. The irreversible semi-derivative peak is asymmetric [3, 4, 65] although the asymmetry is less pronounced as compared with the original voltammetric signal (Fig. 1). For the irreversible case, the peak height (e_p) and the full width at half maximum of the peak, FWHM (w_p) are expressed by Eqs. (4) [3, 4]:

$$e_\mathrm{p} = 0.297An^2\mathrm{F}^2cvD^{1/2}(\mathrm{R}T)^{-1} \quad (4a)$$

$$w_\mathrm{p} = 2.94\mathrm{R}T(n\alpha\mathrm{F})^{-1} \quad (4b)$$

Equation (3) contains an infinite series of exponential terms and is not convenient for data fitting, especially when overlapped signals are considered. It was suggested in [2–4, 65, 66] that an acceptable quality of the fitting of the irreversible semi-derivative peaks may be achieved when a simple function of the same type as Eq. (2) is used (Eq. 5):

$$e = A_1(\cosh(A_2(E-A_3)))^{-2} \quad (5)$$

where A_1, A_2 and A_3 are the fitted coefficients. The e_p and E_p are equal to, respectively, A_1 and A_3, while w_p can be calculated from Eq. (6):

$$w_\mathrm{p} = A_2{}^{-1}\ln\left(\left(\sqrt{2}+1\right)/\left(\sqrt{2}-1\right)\right) = 1.763A_2{}^{-1} \quad (6)$$

One of the main advantages of application of semi-differentiation in analysis of voltammetric data is the possibility of separation of overlapped voltammetric peaks which cannot be deconvoluted correctly using an analysis of voltammetric curves. There are several advantages of deconvolution of overlapped peaks by means of analysis of semi-derivative signals over the fitting of the whole voltammetric curve:

- Semi-derivative peaks are narrower with smaller FWHM as compared with the voltammetric signals. As an example, the FWHM of irreversible semi-derivative peak from Fig. 1 is almost twice smaller than its voltammetric precursor. Application of semi-differentiation improves peaks separation facilitating the deconvolution process. In such case, the accuracy of the peak fitting is better for the semi-derivative curve than for its voltammetric precursor with hardly distinguishable components. Deconvolution by fitting whole voltammetric curves is most effective for bell-shaped voltammetric signals which are easier to separate due to well-defined end and lack of the diffusive tail [2, 67]. Such type of peaks is observed, e.g. surface reactions or processes with finite-space diffusion but not for semi-infinite diffusion discussed in this manuscript.
- Fitting of the whole voltammetric curves is often performed by means of adjusting parameters of simulated curves to the experimental data. The first step of such procedure requires selection of input parameters for simulation, such as the rate constants, diffusion coefficients, concentrations etc. These parameters are then varying in order to reproduce the experimental curve. This approach requires knowledge or assumptions of mechanisms of the processes studied. In contrast, input parameters used in fitting of semi-derivative signals with Eq. (5) or of a similar type are equal to or related to the peak height, peak potential and peak width which are easier to deduce than the parameters describing kinetics of the process.

Application of semi-differentiation for deconvolution of voltammetric peaks is also less complicated than by means of Fourier or wavelet transforms [68–71]. The main disadvantages of the semi-derivative analysis are related to an increase in current noise due to application of differentiation, requirements of subtraction of background currents and formation of artificial semi-derivative signals when the sign of the current does not change when the potential scan is reversed [42, 72].

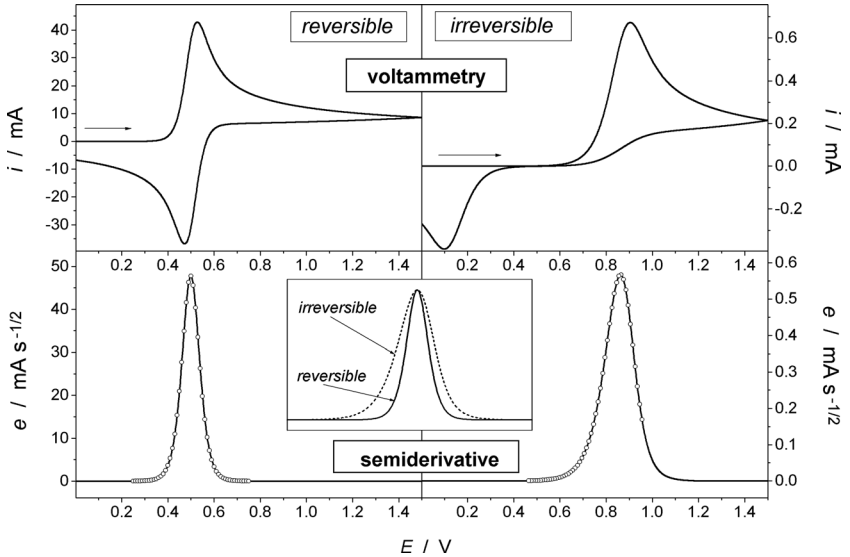

Fig. 1 Simulated voltammetric curves (*top*) and their semi-derivatives (*bottom*) for a reversible (*left*) and an irreversible (*right*) electron transfer. T = 293.15 K, α = 0.5, E° = 0.5 V, c = 0.01 M (irreversible) and 0.5 M (reversible), other parameters used in simulation are given in Table 1. Shown are the first anodic and subsequent cathodic cycles. *Lines in the bottom panels*, simulation with CHI660D software; *open points*, semi-derivatives calculated from Eqs. (2) (reversible) and (3) (irreversible). The *central panel* shows reversible and irreversible semi-derivative peaks with the axis recalculated with the purpose to show their different symmetry

Although much work has been done to evaluate accuracy of deconvolution of reversible peaks by means of fitting semi-derivative curves with Eqs. (2) or (5) (e.g. [2]) it is not clear if overlapped irreversible semi-derivative peaks may be also correctly deconvoluted using Eq. (5) or similar. Although application of Eq. (5) for fitting of irreversible semi-derivative peaks was proposed in the literature [2–4, 65, 66], there are no published, detailed studies showing how accurately electrochemical parameters, such as E_p, e_p and αn, can be determined when irreversible semi-derivative peaks, especially the overlapped ones, are fitted with Eq. (5). The question about accuracy of fitting of the irreversible semi-derivative signals with Eq. (5) is stimulated by the fact that the shape of these signals differs from that predicted by Eq. (5): they are asymmetric while Eq. (5) describes a symmetric signal. It was assumed that the difference between the irreversible semi-derivative peak and its fit with Eq. (5) is small [65, 66], but the accuracy of reproduction of the parameters of such fitted semi-derivative signal was not discussed. Particularly, correctness of parameters of overlapped irreversible semi-derivative peaks which are determined on the basis of fitting with Eq. (5) was not evaluated.

The purpose of this work is to evaluate accuracy of fitting of irreversible semi-derivative peaks with various types of mathematical functions. Apart from Eq. (5), that describes a completely symmetrical semi-derivative signal, two other mathematical equations with included peak asymmetry are also discussed. Simulated voltammetric signals, separated and overlapped, are the subject of the analysis. A special attention is paid to deconvolution of overlapped irreversible semi-derivative signals by means of fitting with discussed mathematical functions. This problem is analysed for various ratios between areas of overlapped peaks separated by various distances.

Calculation

The system subjected to simulation is described by reaction (7):

$$\text{red} \rightarrow \text{ox} + ne^{-}(\text{irreversible}) \text{or red} \leftrightarrow \text{ox} + ne^{-}(\text{reversible}) \quad (7)$$

where *red* and *ox* are the reagents that exist only in the same phase, e.g. as soluble forms in the electrolyte. The other conditions are:

- Transport of the reagents by means of semi-infinite linear diffusion described by the second Fick's law;
- The following criteria of reversibility of the reaction are adopted [73] (Eq. 8):

$$k^0 >> \sqrt{\mathrm{DF}\nu \mathrm{R}^{-1}T^{-1}} \quad \text{(reversible)} \quad (8a)$$

$$k^0 << \sqrt{DF\nu \mathrm{R}^{-1}T^{-1}} \quad \text{(irreversible)} \quad (8b)$$

where k^0 is the standard rate constant of the electrochemical charge transfer.

Table 1 Parameters used for simulation of voltammetric curves for irreversible and reversible systems, the exact values of the parameters of multiple choices (T, α, c and $E°$) are specified for each figure and the electrode area was 1 cm^2

Parameter	Irreversible	Reversible
Temperature (T (K))	278.15–333.15	293.15
Potential scan rate (v (V s^{-1}))	0.1	0.1
Transfer coefficient (symmetry factor; α)	0.1–1	0.5
Standard rate constant (k^0 (cm s^{-1}))	$1{\cdot}10^{-6}$	1
Number of exchanged electrons (n)	1	1
Initial concentration of *red* (M)	0.0020–0.0149	0.01–0.50
Initial concentration of *ox* (M)	0	0
Ox and *red* diffusion coefficient (D (cm^2 s^{-1}))	$1{\cdot}10^{-6}$	$1{\cdot}10^{-6}$
Standard potential ($E°$ (V))	0.200–4.000	0.500–1.398

Simulation of the voltammograms and their processing by means of semi-differentiation was carried out with "Simulation" function of CHI660D electrochemical software (CHInstruments) (fast implicit finite difference algorithm). A comparison with data obtained by application of formulae (2) and (3) taken from [4] confirmed correctness of such performed simulation and semi-differentiation procedures (Fig. 1). The values of the parameters used in the simulation are given in Table 1, the exact values of T, α, c and $E°$ are specified in the captions to respective figures or in the tables. The non-linear least square data-fitting procedure was carried with the MicrocalOrigin software (Levenberg–Marquardt algorithm). The best fit was selected as the one represented by the lowest value of χ^2 obtained for various tested sets of initial (guess) values of the fitted coefficients. The simulated data are noise free and can be considered a case with an excellent peak to noise ratio.

The most accurate way to express asymmetry of a peak is by application of two separate mathematical equations for ascending and descending sections of the signal (split functions) [48, 74, 75]. This procedure, however, is not very convenient since requires a very careful selection of the fitting constraints. Further on, this method can be applied only when separation between peaks is sufficient for determination of E_p's, which is the point where the functions are to be joined, and for defining shapes of ascending and descending sections of the signals. Finally, the relation between widths of ascending and descending sections of the asymmetric peaks predicted by Eq. (3) must be implemented in split functions used for fitting irreversible semi-derivative peaks. Therefore, application of a single mathematical function that satisfactorily expresses asymmetry of the whole peak may facilitate data-fitting process. In this manuscript, it is proposed that asymmetric semi-derivative peaks can be fitted with one of the following formulae: with Eq. (9) or with Eq. (10):

$$e = B_1\left(\cosh\left(B_2\left(E^{B_3} - B_4\right)\right)\right)^{-2} \tag{9}$$

$$e = 4C_1\left(\exp\left(C_2(E - C_3)\right) + \exp\left(-C_4(E - C_3)\right)\right)^{-2} \tag{10}$$

where $B_{1\ldots4}$ and $C_{1\ldots4}$ are the fitted coefficients. C_3 may be both positive and negative while the other coefficients must be positive. The above equations are the modified forms of Eq. (5); equation similar to Eq. (10) has been applied in physics for fitting various asymmetric peak-shaped signals (e.g. [76]). The exponent B_3 in Eq. (9) may have a non-integer value, and this equation can be applied only for positive electrode potentials. This problem, however, can be easily overcome when the potential scale is shifted positively due to addition of an arbitrarily value.

Asymmetry of the semi-derivative peak depends on coefficients B_3 in Eq. (9) and C_2 and C_4 in Eq. (10). Under the conditions of complete symmetry of the peak, i.e. $B_3 = 1$ and $C_4 = C_2$, the Eqs. (9) and (10) are transformed into the ones with the form of (2) or (5), the introduction of multiplication by 4 in Eq. (10) allows equalling C_1 with A_1 from Eq. (5) when $C_4 = C_2$. Thus, an analysis of B_3 value and C_2/C_4 ratio can deliver information about whether the system is irreversible or reversible when the other methods of its evaluation, such as analysis of potential scan rate influence on voltammograms or comparison of oxidation and reduction currents, are not possible to apply.

Equation (3) predicts a strict correlation between the widths of the ascending and descending sections of the irreversible semi-derivative peaks (Fig. 1). This correlation will be maintained also in the peaks obtained by fitting only, when the adequate relationships between the fitted parameters are introduced. Numerous simulated irreversible semi-derivative peaks were subjected to the fitting with Eqs. (9) or (10) in order to find such a relationship between the parameters which affect the peak width and asymmetry, i.e. $B_{2\ldots4}$ (Eq. 9) or $C_{2\ldots4}$ (Eq. 10). The fitting procedure was applied to the peaks with a wide range of E_p's and FWHM's and simulated for various values of $E°$, α and T. An analysis of such obtained $B_{2\ldots4}$ (Eq. (9)) or $C_{2\ldots4}$ (Eq. (10)) datasets was performed in order to find the best correlation between the fitted parameters from each of the equations which reproduces the relationship between widths of both sections of the semi-derivative peaks predicted by Eq. (3). It was found that:

– The relation between B_3, B_2 and B_4 (Eq. 9) can be described by Eq. (11) (Fig. 2a):

$$\ln\left(\frac{B_3}{B_2}\right) = 1.040\ln(B_4) - 0.552 \quad (11)$$

This relation holds for $278.15 \le T \le 333.15$ K; $0.1 \le \alpha \le 1$ and E_p range ca. 0.2–4 V. Combining Eqs. (9) and (11), one gets (12):

$$e = B_1\left(\cosh\left[\left(E^{B_3} - B_4\right)B_3\left(\exp(0.552 - 1.040\ln(B_4))\right)\right]\right)^{-2} \quad (12)$$

– The ratio between C_2 and C_4 (Eq. 10) can be considered constant and equal to 1.544 for $278.15 \le T \le 333.15$ K; $0.1 \le \alpha \le 1$ and E_p range −3 to 3 V (Fig. 2b). Equation (10) can be then transformed to (13):

$$e = 4C_1\left(\exp(1.544C_4(E - C_3)) + \exp(-C_4(E - C_3))\right)^{-2} \quad (13)$$

Equations (12) and (13) are the final forms of mathematical formulae which correctly describe the relationship between ascending and descending sections of an irreversible semi-derivative peak. Application of Eqs. (12) or (13) allows reducing number of adjustable parameters from four (Eqs. 9 and 10) to only three, which is the minimum number of independent parameters describing any voltammetric peak (peak height, potential and width). The irreversible semi-derivative peaks may be then fitted with Eq. (12) or (13); the results obtained for both equations can be directly compared when the positive side of the potential scale is considered. In the case of negative peak potentials an addition of an arbitrary potential value allows shifting the signals to the positive side of the potential scale so the results of fitting with Eq. (12) and Eq. (13) can be also compared.

Formulae describing E_p, e_p and w_p derived from Eqs. 12 and 13 are listed in Table 2 while Eq. (13c) was deduced on the basis of Fig. 3. It was found that variation of $E°$ from −3.362 V ≤ to ≤2.638 V (−3 V ≤ E_p ≤ 3 V) when α and T are fixed leads to ln(C_4) changes not greater than 0.4 %. Thus, when the w_p is plotted vs. ln(C_4) for a wide range of α and T (Fig. 3), the influence of $E°$ (or, simultaneously E_p) on ln(C_4) is practically not detected and the plot can be represented by a straight line given by Eq. (13c). The error in determination of w_p due to E° influence on C_4 is well below 1 %. In general, it was also found that for the wide range of E_p (ca. −4 to 4 V for Eq. 12 and −3 to 3 V for Eq. 13), the errors in determination of E_p, e_p, αn and the peak area does not vary with E_p by more than ca. 1 percentage point or 1 mV in the case of E_p for both Eqs. (12) and (13) (results not shown).

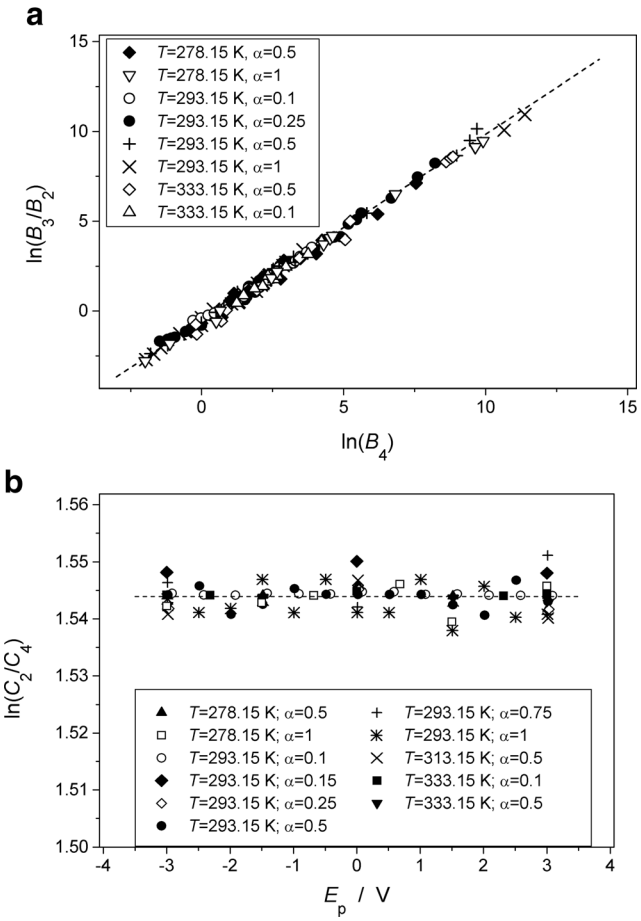

Fig. 2 Relationships between fitting coefficients obtained from fitting of a single irreversible semi-derivative peak with Eq. (12) or (13). α and T used in the simulation are indicated on the plot, other simulation conditions, except $E°$, are the same as for the irreversible case from Fig. 1. $E°$ varies in a wide range from ca. 0.2 to 4 V giving peaks with various values of E_p, the exact range of $E°$ depends on α and T. **a** ln(B_3/B_2) vs. ln(B_4) plot for Eq. (12), the plot covers E_p range from ca. −4 to ca. 4 V. **b** C_2/C_4 vs. the peak potential plot for Eq. (13)

It should be stressed that Eqs. (12)–(13) can be applied only to the asymmetric irreversible peaks and cannot be used for correct fitting of reversible semi-derivative signals. The proposed fitting procedure may start with evaluation of reversibility of the system by means of application of Eq. (9) or (10) and an analysis of obtained B_3 or C_2/C_4 values. When conditions of the peak symmetry are met and the charge transfer can be considered reversible, Eq. (2) can be used, otherwise, Eq. (12) or (13) is to be applied. Application of Eqs. (12) and (13) has several advantages over application of Eqs. (9) and (10) because in the latter cases the widths of the descending and ascending sections of the peaks may vary freely. As a result, the accuracy of determination of the electrochemical parameters (E_p, e_p, αn) of overlapped peaks is higher for Eqs. (12) and (13).

Table 2 Expressions for the peak potential (E_p), the peak height (e_p) and the peak width (w_p) for an irreversible semi-derivative peak derived from Eqs. 12 and 13

Parameter	Derived from Eq. 12	Derived from Eq. 13
E_p (V)	$E_p = {B_4}^{1/B_3}$ (12a)	$C_3 - \frac{0.171}{C_4}$ (13a)
e_p ($As^{-1/2}$)	B_1 (12b)	$1.047C_1$ (13b)
w_p (V)	$\left(\frac{0.881}{\exp(\ln(B_3)+0.552-1.040\ln(B_4))}+B_4\right)^{1/B3}-\left(B_4-\frac{0.881}{\exp(\ln(B_3)+0.552-1.040\ln(B_4))}\right)^{1/B3}$ (12c)	$\exp(-\ln(C_4)+0.353)$ (13c)

Results and discussions

Figures 4 and 5 show results of fitting of a single semi-derivative peak with Eq. (5) (Fig. 4), that describes a completely symmetrical signal, and Eqs. (12) (Fig. 5a) and (13) (Fig. 5b) which are derived for the asymmetric peaks. All the fitting coefficients were set free to vary. The preliminary test of the peak symmetry based on fitting with Eqs. (9) and (10) gives B_3 and C_2/C_4 values of 2.145 and 1.544, respectively, indicating that the peak is not symmetric and the charge transfer process cannot be considered reversible. This justifies application of Eqs. (12) and (13) in the main stage of the fitting process. The advantage of Eqs. (12) and (13) over Eqs. (9) and (10) is that the former formulae give the ratio between the widths of ascending and descending sections of the peak equal to that predicted by Eq. (2) and do not allow free variation of this parameter. Thus, correct fit with Eq. (12) or (13) indicates that the reaction model described by Eq. (2) is applicable to the system studied. In contrast, Eqs. (9) and (10) allow free variation of the abovementioned ratio so the peak perfectly fitted with these equations does not have to meet conditions of the reaction model described by Eq. (2).

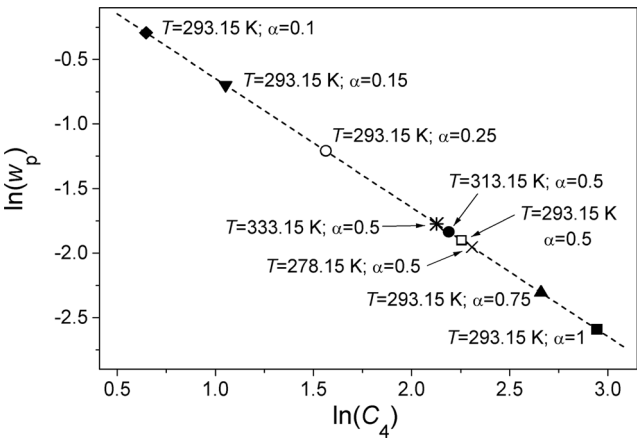

Fig. 3 FWHM of an irreversible semi-derivative peak (w_p) obtained from fits with Eq. (13) as a function of C_4. Data for c = 0.01 M and various T and α indicated on the plot. For each T and α, the $E°$ is in the range from −3.362 to 2.638 V (−3 V ≤ E_p ≤ 3 V), and for various $E°$, the values of ln(C_4) are separated by distances smaller than the size of the points. Other parameters used in the simulation are given in Table 1

The residual distribution seen in Figs. 4 and 5 indicates that the worse quality of the fit is obtained for Eq. (5) with the residuals as high as up to 20 % observed already not far from the peak maximum. Although also for Eqs. (12) and (13), the fits cannot be considered ideal these two equations give a significantly better fit quality with residuals as high as 30 % seen only when the peak onsets are approached at potentials shifted towards the outside of the peak by at least 30 mV as compared with the same residual values obtained for Eq. (5). Table 3 compares values of the relevant electroanalytical parameters used in the simulation with these calculated on the basis of obtained $A_{1\ldots 3}$, $B_{1\ldots 4}$ and $C_{1\ldots 4}$ values. The parameters include:

- The peak potential (E_p) calculated from Eq. (12a) (fit with Eq. 12) or Eq. (13a) (fit with Eq. 13) or equal to A_3 when Eq. (5) is used;
- The peak height (e_p) equal to A_1 for Eq. (5) or calculated from Eqs. (12b) or (13b);
- The product of αn calculated from Eq. (4b) combined with Eqs. (6), (12c) or (13c), for fitting with Eq. (5), (12) and (13), respectively.

An analysis of Table 3 indicates that for a single irreversible derivative peak the values of E_p, e_p, αn obtained by fitting with any of the equations discussed are usually in very good agreement with the values used in the simulation. The accuracy is usually better than 1 % or not worse than 1 mV in the case of E_p. The only exception is E_p obtained from Eq. (5) that differs from the simulated value by 5 mV, a value greater than term $0.055RT(\alpha nF)^{-1}$ in the exponent in Eq. (3). One may assume then that application of any of the discussed equations is appropriate for determination of electroanalytical parameters of a single peak although the residuals distribution and the peak shape reproduction are significantly better for Eqs. (12) and (13).

Figure 6a, b shows anodic sections of voltammetric curves composed with overlapped peaks, together with the respective semi-derivative signals. The curves are composed of peaks from the following processes:

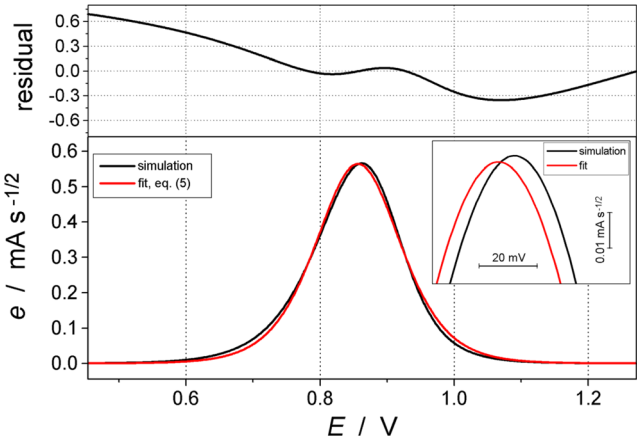

Fig. 4 Results of fitting of a single irreversible semi-derivative peak with Eq. (5). *Bottom panel*, semi-derivative peak with fits; top panel: respective fitting residuals defined as (*e*(simulated) − *e*(fit))/*e*(simulated). *Black*, simulated semi-derivative peak; *red*, fit with Eq. (5) with all fitted parameters set free to vary. Simulation conditions the same as for the irreversible case from Fig. 1

- Reversible and irreversible and for various α obtained from voltammograms simulated for various values of $E°$, c and α (Fig. 6a). Semi-derivative peaks with various FWHM but similar areas are obtained.
- With the same αn and FWHM and the same or various concentrations of the reacting species obtained by varying $E°$ and c in simulated voltammograms (Fig. 6b). Obtained semi-derivative peaks differ in respect to the position and/or area.

Although the number of constituting peaks can be deduced from the voltammograms, only the peak potentials can be directly obtained with acceptable accuracy, determination of the peak height and FWHM requires deconvolution of the respective signals. The peaks seen on semi-derivative curves are also overlapped but due to their bell-like shapes their ends are easier to distinguish as compared to the original voltammetric curves. This is especially clear for peak VI (Fig. 6b), which is hardly seen on the voltammetric curve but becomes clearly distinguishable after the semi-differentiation. Clearly, in this case the accuracy of the peak fitting must be better for the semi-derivative curve than for its voltammetric precursor with hardly distinguishable components. Thus, further analysis of such overlapped semi-derivative signals requires deconvolution by means of fitting with appropriate mathematical functions.

Semi-derivatives are additive [2] and the total e value, e_{total}, is equal to the sum of e of all peaks (14):

$$e_{\text{total}} = \sum_{j=1}^{m} f_m(E) \tag{14}$$

where m is the number of the semi-derivative peaks to be fitted and $f_m(E)$ is the fitting function. It is assumed that for all irreversible peaks the same type of $f_m(E)$ is used. The $f_m(E)$ is given by:

- Equation (5) for both irreversible (asymmetrical) and reversible (symmetrical) peaks. Due to the same general mathematical forms of Eqs. (2) and (5), it is not possible to evaluate reversibility of the process based on the fitting results only. Application of additional tests, such as analysis of potential scan rate influence on peak potentials, is then required to distinguish reversible and irreversible charge transfer processes. The parameters of the reversible peak are calculated by comparing Eqs. (5) and (2).

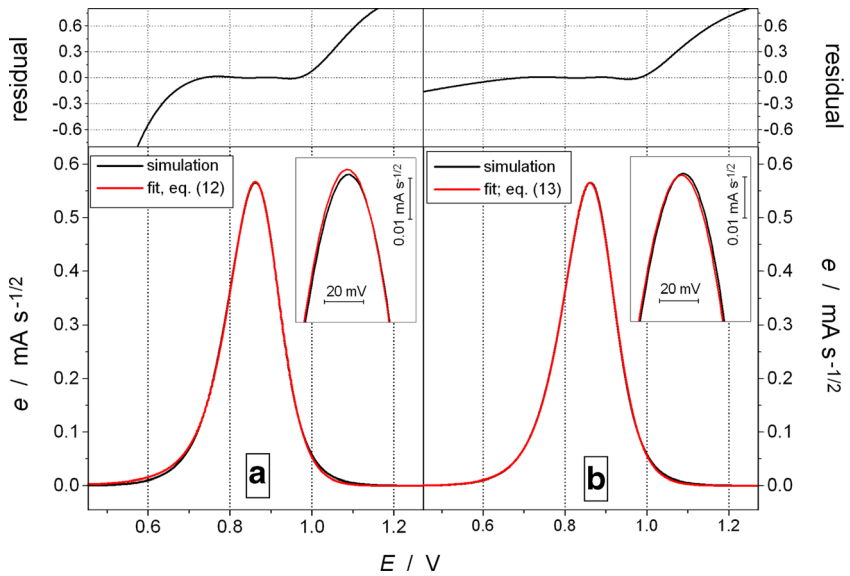

Fig. 5 Results of fitting of a single simulated irreversible semi-derivative peak from Fig. 4 with Eqs. (12) (**a**) and (13) (**b**) with all fitted parameters set free to vary. *Bottom panels*, semi-derivative peak with fits; *top panels*, fitting residuals defined in the same way as for Fig. 4

Table 3 Electroanalytical parameters obtained from fitting of a single irreversible semi-derivative peak with Eqs. (5), (11) and (12) (data from Figs. 4 and 5a, b)

Parameter	Simulation	Fit		
		Equation (5) (Fig. 4)	Equation (12) (Fig. 5a)	Equation (13) (Fig. 5b)
E_p (V)	0.862	0.857	0.862	0.861
$\|\Delta(E_p)\|$ (mV)	–	5	0	1
e_p (mA $s^{-1/2}$)	0.566	0.564	0.567	0.565
$\|\Delta(e_p)\|$ (%)	–	0.353	0.177	0.177
αn	0.500	0.496	0.501	0.497
$\|\Delta(\alpha n)\|$ (%)	–	0.800	0.200	0.600
Peak area (VμA $s^{-1/2}$)	96.476	95.885	96.798	96.114
|Δ(peak area)| (%)	–	0.613	0.334	0.375
χ^2	–	$7.539 \cdot 10^{-11}$	$1.020 \cdot 10^{-11}$	$2.223 \cdot 10^{-12}$

$\Delta(E_p)$ is defined as E_p(simulation)-E_p(fit), $\Delta(e_p)$, $\Delta(\alpha n)$ and Δ(area) are defined as ((parameter (simulation) − parameter (fit))/parameter (simulation))·100 %. Fit qualities expressed as χ^2 are also given

– Asymmetric functions (12) or (13) are used for the irreversible signals while Eq. (2) is used for the reversible ones. All irreversible peaks are fitted with only one function, i.e. (12) or (13); fitting of overlapped signals using Eq. (12) for some of the peaks and Eq. (13) for other signals is not recommended because different ranges of potentials where the functions can be applied, i.e. only positive potentials for Eq. (12), may lead to wrong interpretation of the results. Reversible and irreversible signals may be distinguished in the same way as it was done for a single peak (Fig. 5), i.e. on the basis of B_3 and C_2/C_4 values obtained from preliminary tests with Eqs. (9) or (10) taken as $f_m(E)$ for all the peaks. It should be stressed, however, that the reversibility test based on application of Eqs. (9) or (10) can be applied only when at least a fraction of ascending and descending sections of both overlapped peaks is visible. This is applicable for peaks II and III from Fig. 6a, for which at least a fraction of the ascending and descending sections of both peaks is clearly seen. Only then the ratio between widths of ascending and descending sections of each of the signals can be correctly determined and expressed by B_3 or C_2 and C_4 values. An opposite situation is observed for the peaks overlapped so strongly that some sections of the signals cannot be seen or easily deduced, such as peaks IV and V in Fig. 6b. Under such conditions the widths of the descending section of the first peak and the ascending part of the subsequent signal obtained with Eqs. (9) and (10) may vary freely together with respective B_3 and C_2/C_4 values. Evaluation of the process reversibility on the basis of such obtained coefficients cannot be then considered conclusive. Finally, it should be also stressed that Eq. (12) or (13) give significantly more accurate values of E_p, e_p and αn as compared to Eqs. (9) and (10), even if χ^2 values obtained for both types of Eqs. (9)/(10) and (12)/13) are comparable.

An inspection of Fig. 6 indicates that all three equations reproduce the shape of the semi-derivative signal fairly well and all the features of the original curve are seen also on the fits. A comparison of E_p, e_p and αn obtained from the fitting procedure with the values of the simulated signal allows evaluation of the actual quality of the fit. The results are collected in Table 4; the errors of the calculated values are reported in Table 5.

An analysis of B_3 and C_2/C_3 values from Table 4 shows that only peak III can be considered a reversible one, in agreement with the simulation. Tables 4 and 5 also indicate that the accuracy of determination of E_p, e_p, αn and the peak area is usually better when Eq. (12) or (13) is used instead of Eq. (5) even if χ^2 values are better for Eq. (5). This is especially evident for strongly overlapped peaks, such as these from Fig. 6b, when application of Eq. (5) leads to determination of αn with errors as high as 12–28 %, while for Eqs. (12) and (13), the errors below 4 % are obtained. A similar effect is observed for the peak area although in some cases the e_p can be determined with higher accuracy when Eq. (5) is used.

Several factors have an impact on accuracy of determination of E_p, e_p, αn and the peak area of the overlapped irreversible semi-derivative peaks. Figures 7 and 8 show how this accuracy is influenced by the separation of two peaks of the same size (such as peaks IV and V from Figs. 6b and 7) and by the ratio of the areas of two peaks with a fixed distance between the signals (such as peaks V and VI from Figs. 6b and 8). The plots start with the peak separation of ca. 50–67 % of FWHM (equal to 149 mV in the case of Fig. 7) which is the lowest peak distance

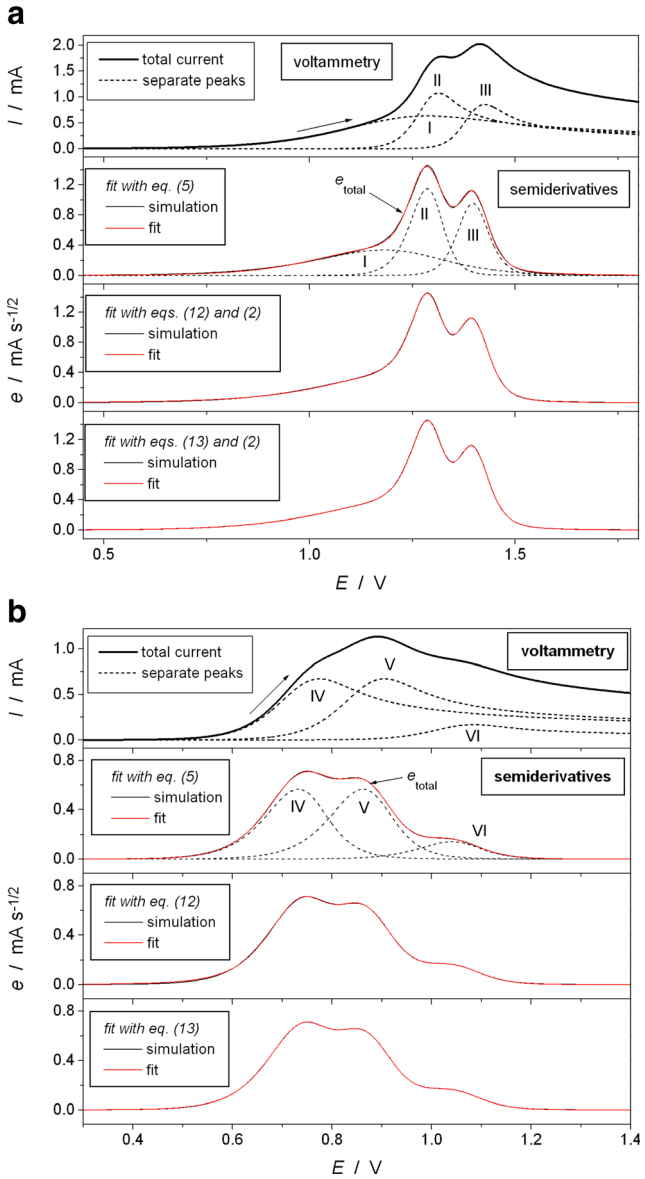

Fig. 6 *Upper panels*, anodic sections of voltammetric curves containing overlapped peaks; *lower panels*, respective semi-derivatives with fits to Eqs. (5), (12) and (13). The semi-derivative curves subjected to the fitting are composed with reversible and irreversible peaks with various FWHM (**a**) and with peaks with the same FWHM and different or the same size (**b**). The separate semi-derivative peaks constituting the total curve are shown only on the first panel with the semi-derivative curve. Simulation conditions together with the results of data fitting are given in Table 4; errors in determination of the electrochemical parameters are reported in Table 5. The reversible peak III from (**a**) was fitted with Eq. (2) while irreversible peaks I and II were fitted with Eq. (12) ("fits with Eq. (2) and (12)") or Eq. (13) ("fits with Eq. (2) and (13)")

allowing conclusion that there is more than one peak after an visual inspection only (Fig. 7), and with the smaller peak constituting 5 % of the main signal, whose existence is still possible to detect visually (Fig. 8). The error plots shown in Fig. 7 are not monotonic due to the fact that for a single peak the distribution of the fitting residuals is potential dependent (cf. Figs. 4 and 5).

In general, the accuracy of determination of E_p, e_p, αn and the peak area increases with the peak separation and with decreasing difference between the peak areas. The accuracy is usually better for Eqs. (12) and (13) than for Eq. 5, the effect especially evident for the lowest separation between the peaks (Fig. 7) and the highest difference in the peak areas (Fig. 8). The strongest influence of the selection of the fitting function is observed for αn. When Eq. (5) is applied, the error in determination of αn may reach several tens of percents, while for Eqs. (12) and (13), the accuracy is not worse than 8 %, i.e. almost an order of magnitude better, even for the smallest separation between the peaks and the highest difference between the peak areas. This comparison indicates that application of symmetric Eq. (5) may lead to incorrect determination of the number of the electrons participating in the reaction in question. Thus, application of Eqs. (12) and (13) for fitting overlapped irreversible semi-derivative peaks is recommended over Eq. (5). Equation (12) gives slightly better accuracy of αn for separated peaks and overlapped peaks with significant difference in size while Eq. (13) gives more accurate values of the maxima and areas of overlapped peaks, is more convenient in use since can be applied also for a negative potential scale and gives slightly better reproducibility of the shape of the semi-derivative curves, as follows from a comparison of χ^2 values.

It should be stressed that the case with two overlapped peaks of the same shape and size shown in Fig. 7 is probably the most difficult one for the reliable deconvolution. It was concluded in [2] that the smallest distance between two overlapped reversible semi-derivative peaks for which deconvolution leads to correct results is slightly greater than FWHM. Similarly, overlapped Gaussian peaks of the same size and the peaks separation smaller than the FWHM cannot be correctly deconvoluted and obtained errors strongly increase for the peaks separation below then the FWHM [77, 78]. Figure 7 indicates that the smallest distance between overlapped irreversible semi-derivative peaks of the same size and shape which allows correct separation of the signals by means of fitting with Eq. (12) or (13) is very similar to the abovementioned cases of reversible semi-derivatives and Gaussian signals and is close to FWHM. For smaller peak separation, the existence of more than one signal cannot be concluded on the basis of a visual inspection.

A different situation is observed when the two overlapped irreversible semi-derivative peaks differ in respect to the shape, such as e.g. peaks I and II from Fig. 6a (FWHM difference of 300 %). In this case, both signals may be separated even when the peak potentials are the same. The errors obtained under such conditions for

Table 4 Fitting coefficients (B_3, C_2 and C_4) and the electroanalytical parameters obtained from fits shown in Fig. 6a (peaks I, II and III) and 6b (peaks (IV, V and VI)

Peak	Equation	B_3 (Eq. (9))	C_2/C_4 (Eq. (10))	E_p (V)	e_p (mA $s^{-1/2}$)	αn or n	Area (V μA $s^{-1/2}$)
I (irreversible): $E°$ = 0.332 V; c = 0.0149 M	Simulation	–	–	1.182	0.338	0.200	143.73
	Fit: (9) or (10)	1.645	1.380	–	–	–	–
	Fit: (5)	–	–	1.172	0.342	0.195	147.97
	Fit: (12)	–	–	1.185	0.339	0.199	146.09
	Fit: (13)	–	–	1.184	0.340	0.196	146.15
II (irreversible): $E°$ = 1.053 V; c = 0.0127 M	Simulation	–	–	1.286	1.148	0.800	122.54
	Fit: (9) or (10)	0.770	1.791	–	–	–	–
	Fit: (5)	–	–	1.285	1.150	0.752	128.86
	Fit: (12)	–	–	1.286	1.140	0.796	121.90
	Fit: (13)	–	–	1.286	1.141	0.796	121.20
III (reversible): $E°$ = 1.398 V; c = 0.01 M	Simulation	–	–	1.397	0.954	1.000	96.49
	Fit: (9) or (10)	1.041	1.032	–	–	–	–
	Fit: (5)	–	–	1.400	0.906	1.075	85.11
	Fit: (2)/(12)	–	–	1.398	0.954	1.010	95.35
	Fit: (2)/(13)	–	–	1.397	0.952	1.012	95.03
IV (irreversible): $E°$ = 0.500 V; c = 0.01 M	Simulation	1.401	1.392	0.732	0.566	0.500	96.48
	Fit: (5)	–	–	0.740	0.652	0.438	125.41
	Fit: (12)	–	–	0.732	0.570	0.511	95.70
	Fit: (13)	–	–	0.733	0.585	0.492	100.57
V (irreversible): $E°$ = 0.370 V; c = 0.01 M	Simulation	0.703	1.197	0.862	0.566	0.500	96.48
	Fit: (5)	–	–	0.872	0.473	0.578	68.94
	Fit: (12)	–	–	0.862	0.572	0.505	97.00
	Fit: (13)	–	–	0.864	0.557	0.517	91.09
VI (irreversible): $E°$ = 0.679 V; c = 0.0025 M	Simulation	1.546	1.286	1.041	0.141	0.500	24.12
	Fit: (5)	–	–	1.040	0.142	0.641	22.44
	Fit: (12)	–	–	1.040	0.148	0.497	25.51
	Fit: (13)	–	–	1.039	0.148	0.492	25.47

αn is for the irreversible peaks while n is for the reversible peak III. Equations (2)/(12) and (2)/(13) indicate that the reversible peak III was fitted with Eq. (2) while two other irreversible signals (I and II) were fitted with Eq. (12) or (13), respectively. The fit qualities, expressed as χ^2, are $3.864 \cdot 10^{-11}$ (Eq. 5); $1.004 \cdot 10^{-11}$ (Eq. 2/12) and $1.085 \cdot 10^{-11}$ (Eq. 2/13) for overlapped peaks I, II and III from Fig. 6a and $2.895 \cdot 10^{-12}$ (Eq. 5); $5.129 \cdot 10^{-12}$ (Eq. 12) and $3.374 \cdot 10^{-13}$ (Eq. 13) for overlapped peaks IV, V and VI from Fig. 6b. The $E°$ and c values used in the simulation are given for each peak; the values of the other parameters are given in Table 1

Eqs. (12) and (13) are not greater than 2 % (or 2 mV for the peak potential). In contrast, Eq. (5) leads to E_p errors as high as 20 mV. A visual inspection of such overlapped semi-derivative signals allows conclusions that the total semi-derivative signal contains more than one peak (results not shown).

One of the well-known drawbacks of the semi-differentiation procedure is increase in the current noise upon its application [2, 42, 72]. Although this effect might complicate deconvolution of overlapped semi-derivative signals leading to higher errors, the presence of current noise should have the same impact for all the equations discussed above, i.e. (5), (12) and (13). Therefore, the conclusions drawn from the comparison of results of application of Eqs. (5) and (12) or (13) should be valid also when the current noise is present.

The analysis reported in this manuscript is limited to two extreme systems: completely reversible and irreversible. When a signal cannot be fitted satisfactorily with any of Eq. (5), (12) or (13), the system can be considered the one which does not meet requirements of complete reversibility nor irreversibility. Thus, the process may be quasi-reversible or the processes studied cannot be described by discussed model with a charge transfer and semi-infinite diffusion. The

Table 5 Errors of E_p, e_p, αn (or n), and the peak area obtained from Fig. 6a (peaks I, II and III) and 6b (peaks IV, V and VI) and Table 4

Peak	Equation	$\lvert\Delta(E_p)\rvert$ (mV)	$\lvert(\Delta e_p)\rvert$ (%)	$\lvert\Delta(\alpha n)\rvert$ (irreversible) or $\lvert\Delta(n)\rvert$ (reversible) (%)	$\lvert\Delta$(area)$\rvert$ (%)
I (irreversible)	Fit: (5)	10	1.183	2.500	2.950
	Fit: (12)	3	0.296	0.500	1.642
	Fit: (13)	2	0.592	2.000	1.684
II (irreversible)	Fit: (5)	1	0.174	6.000	5.158
	Fit: (12)	<1	0.697	0.500	0.522
	Fit: (13)	<1	0.610	0.500	1.094
III (reversible)	Fit: (5)	3	5.031	7.500	11.794
	Fit: (2)/(12)	1	0.105	$<10^{-3}$	1.181
	Fit: (2)/(13)	<1	0.210	1.200	1.513
IV (irreversible)	Fit: (5)	8	15.300	12.335	29.987
	Fit: (12)	<1	0.780	2.222	0.802
	Fit: (13)	1	3.367	1.627	4.241
V (irreversible)	Fit: (5)	10	16.410	15.619	28.548
	Fit: (12)	<1	1.001	0.937	0.537
	Fit: (13)	2	1.555	3.445	5.589
VI (irreversible)	Fit: (5)	1	0.705	28.275	6.950
	Fit: (12)	1	4.892	0.534	5.756
	Fit: (13)	2	4.847	1.507	5.599

The errors are defined in the same way as for Table 3. Equations (2)/(12) and (2)/(13) indicate that the reversible peak III was fitted with Eq. (2) while for two other irreversible signals Eq. (12) or (13) was used, respectively

papers devoted to this topic focus mainly or exclusively on completely reversible or irreversible processes. The quasi-reversible systems require separate studies with a careful comparison of obtained results with those coming from application of equations for completely reversible and irreversible cases, especially in terms of analysis of fitting errors.

Conclusions

Voltammetric curves simulated for processes under conditions of semi-infinite linear diffusion and irreversible charge transfer with both reduced and oxidised species dissolved in the electrolyte were analysed by means of

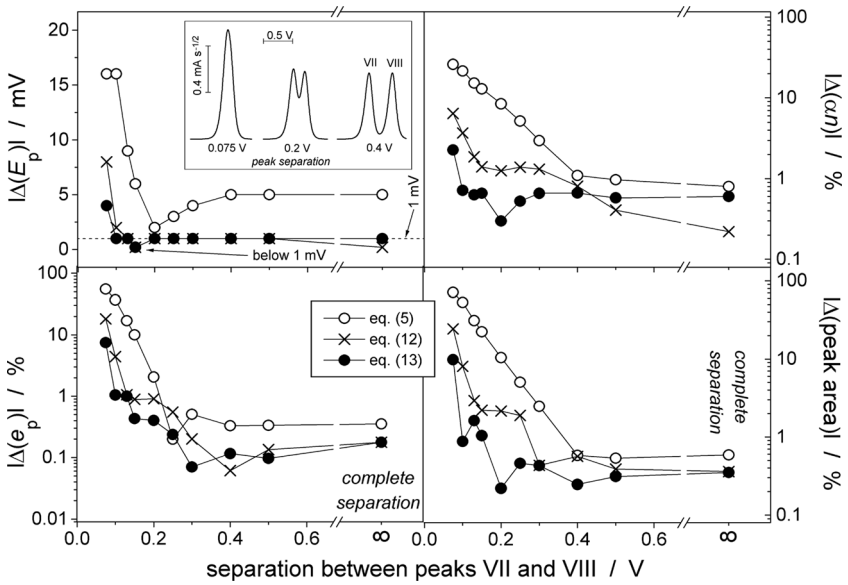

Fig. 7 Average $\lvert\Delta(E_p)\rvert$, $\lvert\Delta(e_p)\rvert$, $\lvert\Delta(\alpha n)\rvert$ and $\lvert\Delta$(peak area)$\rvert$ for fitting of two overlapped semi-derivative peaks (VII and VIII in the inset in the left upper panel) with Eqs. (5), (12) and (13) for various peak separation expressed as a distance between the peaks. The simulation conditions the same as for irreversible case from Fig. 1 except that $E°$ for peak VIII was varied between 0.862 and 1.362 V. The errors are calculated as average values for both deconvoluted peaks, for each separate peak, the errors are defined in the same way as for Table 3; for $\lvert\Delta(e_p)\rvert$, $\lvert\Delta(\alpha n)\rvert$ and $\lvert\Delta$(peak area)$\rvert$ a logarithmic scale is used

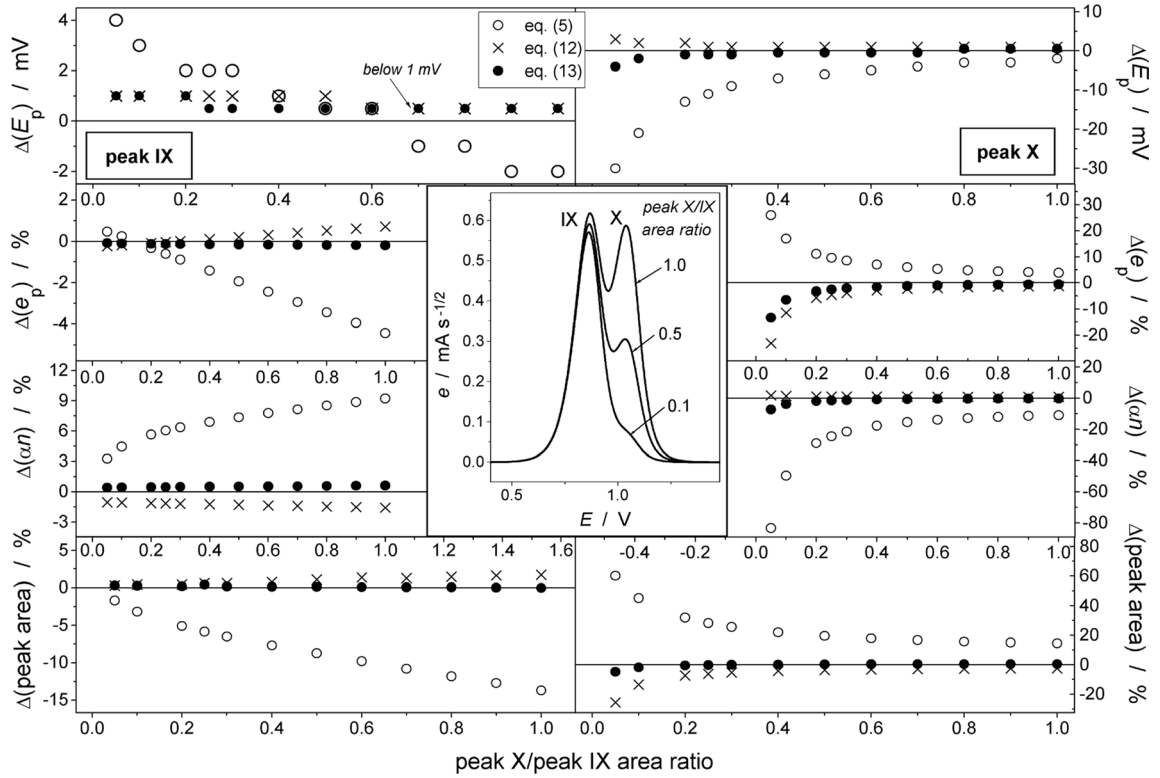

Fig. 8 $\Delta(E_p)$, $\Delta(e_p)$, $\Delta(\alpha n)$ and Δ(peak area) obtained from fitting of two overlapped semi-derivative peaks (*IX and X in the central inset*) with Eqs. (5), (12) and (13) for various ratios of the peak areas. Presented errors are shown for each peak separately and are defined in the same way as for Fig. 7 except that the actual values are shown instead of moduli; $\Delta(E_p)$ values are rounded to 1 mV, and the errors below this value are indicated on the plot. Simulation conditions the same as for the irreversible case from Fig. 1 except that for peak X: $0.500 \le E^\circ$ 0.678 V and $5 \cdot 10^{-4} \le c \le 0.01$ M

semi-differentiation. Semi-differentiation of strongly overlapped voltammetric signals leads to formation of overlapped semi-derivative peaks whose further analysis must involve fitting with appropriate mathematical functions. Several authors suggested that asymmetric semi-derivative peaks obtained for an irreversible electron transfer can be fitted with a mathematical function of the same type as the one used for completely symmetrical semi-derivative signals. This paper compares the results of fitting of the irreversible semi-derivative peaks with several types of mathematical functions: the abovementioned symmetric one and two alternative functions with introduced peak asymmetry (asymmetric functions). The usability of each of the functions was evaluated by means of a comparison of obtained values of the electrochemical parameters, such as peak height, peak potential and the product of number of exchanged electrons and symmetry factor (or transfer coefficient, αn) with the respective values used in simulation. It was found that when the irreversible semi-derivative peaks are fitted with the symmetric function the acceptable accuracy of determination of the abovementioned parameters is obtained only for a single semi-derivative peak or for overlapped semi-derivative peaks with significant differences in their width at half maximum. Application of asymmetric functions peaks has several advantages over the symmetric function. Thus, the latter functions significantly better reproduce the shape of the irreversible semi-derivative signals and give more accurate values of the electrochemical parameters, especially for strongly overlapped peaks. As an example, the error in αn obtained from fitting of overlapped irreversible semi-derivative peaks with a symmetric function may be as high as several tens of percents, a value greater by an order of magnitude than the results of data fitting with the asymmetric functions.

Acknowledgements This work was financially supported by the Ministry of Science and Higher Education (grant no. N N204 125037) and by The Faculty of Chemistry, University of Warsaw (grants no. 120000-501/68-179201 and BST 1763-8).

References

1. Bard AJ, Faulkner L (1980) Electrochemical methods. Fundamentals and applications. Wiley, New York
2. Pałys M, Korba T, Bos M, Van der Linden WE (1991) The separation of overlapping peaks in cyclic voltammetry by means of semi-differential transformation. Talanta 38:723–733
3. Dalrymple-Alford P, Goto M, Oldham KB (1977) Peak shapes in semidifferential electroanalysis. Anal Chem 49:1390–1394
4. Dalrymple-Alford P, Goto M, Oldham KB (1977) Shapes of derivative neopolarograms. J Electroanal Chem 85:1–15
5. Oldham KB, Myland JC (2011) Modelling cyclic voltammetry without digital simulation. Electrochim Acta 56:10612–10625
6. Bobrowski A, Kasprzyk G, Mocák J (2000) Theoretical and experimental resolution of semi-derivative linear scan voltammetry. Collect Czechoslov Chem Commun 65:979–994
7. Goto M, Oldham KB (1976) Semiintegral electroanalysis: the shape of irreversible neopolarograms. Anal Chem 48:1671–1676
8. Myland JC, Oldham KB (2015) How does a reversible electrode respond in a.c. voltammetry? Part 1: an analytic solution for the semiintegral for amplitudes less than 40 Mv. J Electroanal Chem 754:165–172
9. Oldham KB, Myland JC, Bond AM, Mashkina EA, Simonov AN (2014) The aperiodic current, and its semiintegral, in reversible a.c. voltammetry: theory and experiment. J Electroanal Chem 719:113–121
10. Simonov AN, Mashkina E, Mahon PJ, Oldham KB, Bond AM (2015) Determination of diffusion coefficients from semiintegrated d.c. and a.c. voltammetric data: overcoming the edge effect at macrodisc electrodes. J Electroanal Chem 744:110–116
11. Myland JC, Oldham KB (1983) An analytical expression for the current-voltage relationship during reversible cyclic voltammetry. J Electroanal Chem 153:43–54
12. Yu JS, Zhang ZX (1996) Differentiation, semidifferentiation and semi-integration of a digital signals based on Fourier transformations. J Electroanal Chem 403:1–9
13. Goto M, Ishii D (1975) Semidifferential electroanalysis. J Electroanal Chem 61:361–365
14. Keightley AM, Myland JC, Oldham KB, Symons PG (1992) Reversible cyclic voltammetry in the presence of product. J Electroanal Chem 322:25–54
15. Goto M, Oldham KB (1973) Semiintegral electroanalysis: shapes of neopolarograms. Anal Chem 45:2043–2050
16. Barnard GM, Boddington T, Gregor JE, Pettit LD, Taylor N (1990) An investigation into the determination of stability constants of metal complexes by convolution-deconvolution cyclic voltammetry. Talanta 37:219–228
17. Woodard FE, Goodin RD, Kinlen PJ (1984) Kinetic convolution analysis of cyclic voltammetric data. Anal Chem 56:1920–1923
18. Mahon PJ (2009) Convolutive reshaping with applications for voltammetry. J Solid State Electrochem 13:573–582
19. Mahon PJ, Oldham KB (1998) Voltammetric modeling via extended semiintegrals. J Electroanal Chem 445:179–195
20. Oldham KB, Zoski CG (1983) Semiintegral electroanalysis with discrimination against charging current. J Electroanal Chem 145: 265–278
21. Brannan T, Weinberger J, Knott P, Taff I, Kaufmann H, Togasaki D, Nieves-Rosa J, Maker H (1987) Direct evidence of acute, massive striatal dopamine release in gerbils with unilateral strokes. Stroke 18:108–110
22. Ghoneim MM, El-Hallag IS (2010) Electrochemical behavior of hexamethylbenzene isocloso ruthenium-borane complex at a glassy carbon electrode in non-aqueous medium. J Braz Chem Soc 21:7–15
23. El-Hallag IS, Asiri AM, El-Mossalamy EH (2013) Data analysis and evaluation of the electrochemical parameters for the et process via convolutive voltammetry and digital simulation. J Chil Chem Soc 58:1921–1925
24. Prieto I, Pedrosa JM, Martín MT, Camacho L (2000) Numerical determination of extended semi integrals and semi differentials by using spline cubic functions. Applications to an EE reversible mechanism in cyclic voltammetry. J Electroanal Chem 485:7–12
25. İnam R, Bilgin C (2013) Square wave voltammetric determination of methiocarb insecticide based on multiwall carbon nanotube paste electrode. J Appl Electrochem 43:425–432
26. O'Neill RD, Grünewald RA, Fillenz M, Albery WJ (1982) Linear sweep voltammetry with carbon paste electrodes in the rat striatum. Neurosci 7:1945–1954
27. O'Neill RD, Fillenz M, Albery WJ (1983) The development of linear sweep voltammetry with carbon paste electrodes in vivo. J Neurosci Meth 8:263–273
28. Wang MY, Zhang DE, Tong ZW, Xu XY, Yang XJ (2011) Voltammetric behavior and the determination of quercetin at a flowerlike Co_3O_4 nanoparticles modified glassy carbon electrode. J Appl Electrochem 41:189–196
29. Li Y (2009) Fractional-order differentiation of the Gaussian function for processing overlapped peaks. Anal Sci 25:1339–1344
30. Levillain E, Gaillard F, Leghie P, Demortier A, Lelieur JP (1997) On the understanding of the reduction of Sulphur (S_8) dimethylformamide (DMF). J Electroanal Chem 420:167–177
31. Goto M, Kato M, Ishii D (1981) Semidifferential electroanalysis with a solid working electrode. Anal Chim Acta 126:95–104
32. Lane RF, Hubbard AT, Blaha CD (1979) Application of semidifferential electroanalysis to studies of neurotransmitters in the central nervous system. J Electroanal Chem 95:117–122
33. Mo C, Li X (2007) Microstructure and structural transition in coconut oil microemulsion using. J Colloid Interf Sci 312:355–362
34. Cassir M, Moutiers G, Devynck J (1993) Stability and characterization of oxygen species in alkali molten carbonate: a thermodynamic and electrochemical approach. J Electrochem Soc 140:3114–3123
35. Muratov DV, Romanov AS, Loginov DA, Corsini M, Fabrizi de Biani F, Kudinov AR (2015) Dicationic μ-diborolyl arene triple-decker complexes CpCo(μ-1,3-3B2Me5)M(arene).2+ (M = Rh, Ir; Cp = cyclopentadienyl): synthesis, structures, electrochemistry and bonding. Eur J Inorg Chem 5:804–816
36. Klička R (1998) Adsorption in semi-differential voltammetry. J Electroanal Chem 455:253–257
37. Pedrosa JM, Martín MT, Ruiz JJ, Camacho L (2002) Application of the cyclic semi-integral voltammetry and cyclic semi-differential voltammetry to the determination of the reduction mechanism of a Ni–porphyrin. J Electroanal Chem 523:160–168
38. Goto M, Miura Y, Yoshida H, Ishii D (1983) Determination of trace phosphate ion using semidifferential electroanalysis. Mikrochim Acta 79:121–130
39. Tylka MM, Willit JL, Prakash J, Williamson MA (2015) Application of voltammetry for quantitative analysis of actinides in molten salts. J Electrochem Soc 162:H852–H859
40. Matsumiya M, Takagi R, Fujita R (1997) Recovery of Eu^{2+} and Sr^{2+} using liquid metallic cathodes in molten NaCl-KCl and KCl system. J Nucl Sci Tech 34:310–317
41. Chu L, Han L, Zhang X (2011) Electrochemical simultaneous determination of nitrophenol isomers at nano-gold modified glassy carbon electrode. J Applied Electrochem 41:687–694
42. Kasprzyk GP, Jaskuła M (2004) Application of the hybrid genetic-simplex algorithm for deconvolution of electrochemical responses in SDLSV method. J Electroanal Chem 567:39–66
43. Matsumiya M (2016) In: Chen J (ed) Application of ionic liquids on rare earth green separation and utilization. Berlin-Heidelberg, Springer

44. Matsumiya M, Takano M, Takagi R, Fujita R (1999) Electrochemical behavior of Ba^{2+} at liquid metal cathodes in molten chlorides. Z Naturforsch 54A:739–746
45. Al-Owais AA, El-Hallag IS (2016) Electrochemical behaviour of copper(II) at a hanging mercury drop electrode. Sci Asia 42: 114–120
46. Liu YL, Zhou W, Tang HB, Liu ZR, Liu K, Yuan LY, Feng YX, Chai ZF, Shi WQ (2016) Diffusion coefficient of Ho^{3+} at liquid zinc electrode and co-reduction behaviors of Ho^{3+} and Zn^{2+} on W electrode in the LiCl-KCl eutectic. Electrochim Acta 211:313–321
47. Ota H, Matsumiya M, Yamada T, Fujita T, Kawakami S (2016) Purification of rare earth bis(trifluoromethyl-sulfonyl)amide salts by hydrometallurgy and electrodeposition of neodymium metal using potassium bis(trifluoromethyl-sulfonyl)amide melts. Sep Purif Technol 170:417–426
48. Rappleye D, Jeong SM, Simpson M (2016) Electroanalytical measurements of binary-analyte mixtures in molten LiCl-KCl eutectic: gadolinium(III)- and lanthanum(III)-chloride. J Electrochem Soc 163:B507–B516
49. Doménech-Carbó A, Villegas MÁ, Agua F, Martínez-Ramírez S, Doménech-Carbó MT, Martínez B (2016) Electrochemical fingerprint of archeological lead silicate glasses using the voltammetry of microparticles approach. J Am Ceramic Soc. doi:10.1111/jace.14430
50. Goto M, Ikenoya K, Kajihara M, Ishii D (1978) Application of semidifferential electroanalysis to anodic stripping voltammetry. Anal Chim Acta 101:131–138
51. Goto M, Ikenoya K, Ishii D (1979) Anodic stripping semidifferential electroanalysis with thin mercury film electrode formed in situ. Anal Chem 51:110–115
52. Mocak J, Janiga I, Rievaj M, Bustin D (2007) The use of fractional differentiation or integration for signal improvement. Meas Sci Rev 7:39–42
53. Rieger PH (1994) Electrochemistry. Springer, Dordrecht
54. Das S (2011) Functional fractional calculus. Springer, Berlin-Heidelberg
55. Petráš I (2011) In: Assi AH (ed) Engineering education and research using MATLAB, InTech
56. Zoski CG, Bond AM, Colyer CL, Myland JC, Oldham KB (1989) Near-steady-state cyclic voltammetry at microelectrodes. J Electroanal Chem 263:1–21
57. Oldham KB, Spanier J (1970) The replacement of Fick's laws by a formulation involving semidifferentiation. J Electroanal Chem 26: 331–341
58. Li YL, Tang HQ, Chen HX (2011) Fractional-order derivative spectroscopy for resolving simulated overlapped Lorentzian peaks. Chemometr Intell Lab 107:83–89
59. Jin W, Cui H, Zhu L, Wang S (1991) On the theory of the integer and half-integer integral and derivative linear potential sweep voltammetry for a totally irreversible interfacial reaction. J Electroanal Chem 309:37–47
60. Oldham KB (2010) Fractional differential equations in electrochemistry. Adv Eng Soft 41:9–12
61. Myland JC, Oldham KB (2002) A general analytical treatment of modulated linear-ramp voltammetry for reversible processes. J Electroanal Chem 535:27–35
62. Stromberg AG, Romanenko SV, Romanenko ES (2000) Systematic study of elementary models of analytical signals. J Anal Chem 55: 615–625
63. Bockris JO'M, Khan SUM (1993) Surface electrochemistry. A molecular level approach. Plenum Press, New York
64. Bockris JO'M, Nagy Z (1973) Symmetry factor and transfer coefficient: a source of confusion in electrode kinetics. J Chem Edu 50: 839–843
65. Caster DM, Toman JJ, Brown SD (1983) Curve fitting of semiderivative linear scan voltammetric responses: effect of reaction reversibility. Anal Chem 55:2143–2147
66. Toman JJ, Brown SD (1981) Peak resolution by semiderivative voltammetry. Anal Chem 53:1497–1504
67. Huang W, Henderson TLE, Bond AM, Oldham KB (1995) Curve fitting to resolve overlapping voltammetric peaks: model and examples. Anal Chim Acta 304:1–15
68. Jakubowska M (2011) Signal processing in electrochemistry. Electroanalysis 23:553–572
69. Shao X, Pang C, Wu S, Lin X (2000) Development of wavelet transform voltammetric analyzer. Talanta 50:1175–1182
70. Nie L, Wu S, Wang J, Zheng L, Lin X, Lei Rui L (2001) Continuous wavelet transform and its application to resolving and quantifying the overlapped voltammetric peaks. Anal Chim Acta 450:185–192
71. Jakubowska M (2008) Inverse continuous wavelet transform in voltammetry. Chemometr Int Lab Sys 94:131–139
72. Li YL, Tang HQ, Chen HX (2011) Fractional-order derivative spectroscopy for resolving simulated overlapped Lorenztian peaks. Chemometr Int Lab Sys 107:83–89
73. Compton RG, Banks CE (2011) Understanding Voltammetry. Imperial College Press, London
74. Romanenko SV, Stromberg AG, Pushkareva TN (2006) Modeling of analytical peaks: peaks properties and basic peak functions. Anal Chim Acta 580:99–106
75. Dubrovkin J (2016) Mathematical methods for separation of overlapping asymmetrical peaks in spectroscopy and chromatography. Case study: one-dimensional signals. Int J Emerg Techn Comput Appl Sci 11:1–8
76. Sharma AK, Naik PA, Gupta PD (2004) Simple and sensitive method for visual detection of temporal asymmetry of ultrashort laser pulses. Opt Express 12:1389–1396
77. Lu J, Trnka MJ, Roh SH, Robinson PJJ, Shiau C, Galonic Fujimori D, Chiu W, Burlingame AL, Guan S (2015) Improved peak detection and deconvolution of native electrospray mass spectra from large protein complexes. J Am Soc Mass Spectrom 26:2141–2151
78. Cubison MJ, Jimenez JL (2015) Statistical precision of the intensities retrieved from constrained fitting of overlapping peaks in high-resolution mass spectra. Atmos Meas Tech 8:2333–2345